CrystEngComm

Accepted Manuscript

ROYAL SOCIETY
OF CHEMISTRY

www.rsc.org/crystengcomm

Journal Name RSCPublishing

ARTICLE

Cite this: DOI: 10.1039/x0xx00000x

Received 00th January 2012,
Accepted 00th January 2012

DOI: 10.1039/x0xx00000x

www.rsc.org/

Five Cu(I) and Zn(II) clusters and coordination polymers of 2-pyridyl-1,2,3-triazoles: synthesis, structures and luminescent properties

Shi-Qiang Bai,*[a] Lu Jiang,[a] Bin Sun,[b] David James Young[ac] and T. S. Andy Hor*[ab]

Three stair-step $[Cu_4I_4]$ cluster based complexes $[Cu_4I_4(L1)_2]$ (**1**), $[Cu_4I_4(L2)]_n$ (**2**), $[Cu_4I_4(L3)]_n\cdot 2n(CH_3CN)$ (**3**) and two linear Zn(II) coordination polymers $[ZnCl_2(L1)]_n$ (**4**) and $[ZnCl_2(L3)]_n$ (**5**) with 2-pyridyl-triazole ligand (L1 = 2-((4-propyl-1*H*-1,2,3-triazol-1-yl)methyl)pyridine, L2 = 1,3-bis(1-(pyridin-2-ylmethyl)-1*H*-1,2,3-triazol-4-yl)propane and L3 = 1,4-bis(1-(pyridin-2-ylmethyl)-1*H*-1,2,3-triazol-4-yl)butane) have been synthesized and characterized by single-crystal X-ray diffraction (XRD), powder XRD, thermogravimetric analysis and photoluminescence spectroscopy. Complex **1** possesses a stair-step $[Cu_4I_4]$ cluster structure. Complexes **2** and **3** are 1-D polymeric forms of the $[Cu_4I_4]$ clusters. Complexes **4** and **5** are 1-D Zn(II) polymeric structures bridged by L1 and L3 spacers, respectively. In **1**–**3**, ligands L1–L3 adopt a bidentate/monodentate dual coordination mode through cooperation of the triazole and pyridyl nitrogen donors. Ligand L1 exhibits an unusual open-bridging mode in complex **4**, employing N_{py} and 3'-N_{tri} donors. By comparison, ligand L3 bridges two metal centers in complex **5** using 3,3'-N_{tri} donors. The structural effects (4-pyridyl- and 2-pyridyl-triazole) and H-bonding interactions on the coordination structures are described and discussed. All five complexes exhibit solid-state photoluminescence with maximum emissions in the region of 440–490 nm.

Introduction

Luminescent metal complexes have attracted immense attention because of their diverse potential applications and the ability to design and engineer different structures that tune functional activities. These complexes have been used in photoluminescent sensing and detection, biological probes, optoelectronic devices and photocatalysis etc.[1–5] Choice of metal and ligand combinations determines the resultant structure, electronic make-up and activities. A variety of coordination environments with interesting luminescent behaviours have been achieved from different types of ligands with lanthanides and d^{10} transition metal ions.[6,7] Phosphines, N-heterocyclic carbenes and nitrogen-based systems are the most used ligands in this respect.[8–12] Use of the copper-catalyzed azide-alkyne cycloaddition (CuAAC) click reactions enables the synthesis of macrocyclic molecules and polymers, as well as modification of biomolecules, surfaces and nanoparticles.[13–15] The products of CuAAC reactions, such as 1,4-disubstituted 1,2,3-triazoles, have been employed as ligands for catalysts and as building blocks for luminescent metal complexes. These examples illustrate the application of the CuAAC reactions in functional coordination chemistry.[16–23] We recently reported the syntheses of a range of pyridine, pyrazole and benzyltriazole hybridized 1,2,3-triazole ligands from CuAAC reactions. These ligands serve as functional spacers in a range of di- and poly-nuclear frameworks and polymers.[24–29] We herein extend the investigation of using 2-pyridyl-1,2,3-triazoles (Scheme 1) to support luminescent Cu(I) and Zn(II) cluster and polymeric complexes.

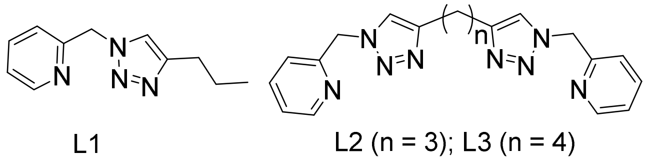

Scheme 1 The structures of ligands L1–L3.

Experimental

General

Sodium azide is potentially explosive. Only micro-scaled reactions may be performed, and all operations must be handled with necessary precautionary measures. All starting chemicals were used as received. Elemental analyses were performed on a thermo electron corporation flash EA 1112 series analyzer. Infrared spectra were obtained on a Perkin Elmer Spectrum 2000 FT-IR spectrometer from samples in KBr disc. Powder X-ray diffraction data were collected on a Bruker D8 Advance X-ray Diffractometer with Cu-Kα radiation (λ = 1.5418 Å). Thermogravimetric analyses (TGA) were carried out in air stream using *TA* Instruments TGA Q500 analyzer with heating rate of 10 °C/min. BET measurement for complex **3** was carried out using micromeritics ASAP 2020 Surface Area and Porosity Analyzer. Photoluminescence was measured using a Perkin Elmer LS55 luminescence spectrometer. During the measurements, an attenuator of 1 % T was used for all the complexes **1–5** due to their strong emissive intensities.

Synthesis

$[Cu_4I_4(L1)_2]$ (**1**). A CH_3CN solution (2 mL) of ligand L1 (0.1 mmol, 20 mg) was layered onto a CH_3CN solution (5 mL) of CuI (0.2 mmol, 38 mg) in a test tube. Slow diffusion of the resulting solution afforded yellow crystals of **1** within one week. Yield: 45 mg, 77 %. Anal. Calcd. for $C_{22}H_{28}Cu_4I_4N_8$ (1166.32): C, 22.66; H, 2.42; N, 9.61%. Found: C, 22.83; H, 2.32; N, 9.66%. Main IR bands (cm^{-1}): 3120m, 2961m, 2928m, 2870m, 1599m, 1539m, 1507m, 1475m, 1459m, 1442m, 1419m, 1308m, 1235m, 1153m, 1054m, 802m, 763s, 667m, 640m and 415m.

$[Cu_4I_4(L2)]_n$ (**2**). A CH_3CN solution (1 mL) of ligand L2 (0.025 mmol, 9 mg) was layered onto a CH_3CN solution (3 mL) of CuI (0.1 mmol, 19 mg) in a test tube. Slow diffusion of the resulting solution afforded yellow crystals of **2** within two weeks. Yield: 24 mg, 85 %. Anal. Calcd. for $C_{19}H_{20}Cu_4I_4N_8$ (1122.19): C, 20.34; H, 1.80; N, 9.99%. Found: C, 20.67; H, 1.79; N, 9.99%. Main IR bands (cm^{-1}): 3120m, 3080m, 2990m, 2914m, 2854m, 1625m, 1595m, 1552m, 1467m, 1443m, 1421m, 1306m, 1258m, 1243m, 1214m, 1149m, 1104m, 1080m, 1050m, 1011m, 808m, 777m, 759m, 676m and 414m.

$[Cu_4I_4(L3)]_n \cdot 2n(CH_3CN)$ (**3**). Complex **3** was prepared using the above method for **2**, but replacing ligand L2 with L3 (0.025 mmol, 9 mg). Yield: 28 mg, 98 %. Anal. Calcd. for as-synthesized sample $[Cu_4I_4(L3)] \cdot 0.7(CH_3CN)$ ($C_{21.4}H_{24.1}Cu_4I_4N_{8.7}$, 1164.99): C, 22.06; H, 2.09; N, 10.46 %. Found: C, 22.23; H, 2.05; N, 10.37 %. Main IR bands (cm^{-1}): 3123m, 3070m, 2986m, 2930m, 2856m, 1632m, 1597m, 1544m, 1471m, 1441m, 1426m, 1307m, 1240m, 1219m, 1152m, 1070m, 1051m, 1012m, 801m, 758m, 714m and 416m.

$[ZnCl_2(L1)]_n$ (**4**). A CH_3OH solution (2 mL) of $ZnCl_2$ (0.1 mmol, 14 mg) was added to a CH_3OH solution (2 mL) of L1 (0.1 mmol, 20 mg). Slow evaporation of the resulting solution afforded colorless crystals of **4** within a week. Yield: 20 mg, 59 %. Anal. Calcd. for $C_{11}H_{14}Cl_2N_4Zn$ (338.54): C, 39.03; H, 4.17; N, 16.55%. Found: C, 39.19; H, 4.26; N, 16.80 %. Main IR bands (cm^{-1}): 3145m, 3089m, 2964m, 2937m, 2875m, 1606m, 1571m, 1557m, 1486m, 1461m, 1443m, 1427m, 1373m, 1360m, 1329m, 1310m, 1292m, 1237m, 1224m, 1190m, 1162m, 1150m, 1103m, 1076m, 1062m, 1024m, 900m, 824m, 796m, 780s, 737m, 707m, 659m, 642m, 606m, 470m, 446m and 420m.

$[ZnCl_2(L3)]_n$ (**5**). A CH_3OH solution (2 mL) of $ZnCl_2$ (0.1 mmol, 14 mg) was added to a CH_3OH solution (2 mL) of L3 (0.1 mmol, 37 mg). Slow evaporation of the resulting solution afforded colorless crystals of **5** within one week. Yield: 45 mg, 60 %. Anal. Calcd. for $C_{20}H_{22}Cl_2ZnN_8$ (510.73): C, 47.03; H, 4.34; N, 21.94%. Found: C, 46.80; H, 4.27; N, 22.10 %. Main IR bands (cm^{-1}): 3132m, 3087m, 2952m, 2934m, 2865m, 1598m, 1589m, 1573m, 1556m, 1481m, 1456m, 1433s, 1372m, 1351m, 1276m, 1231m, 1183m, 1157m, 1090m, 1053m, 997m, 819m, 808m, 768m, 758s, 727m, 683m, 627m, 596m and 461m.

X-ray diffraction

Table 1 Summary of crystallographic data for **1–5**

Complex	**1**	**2**	**3**	**4**	**5**
Formula	$C_{22}H_{28}Cu_4I_4N_8$	$C_{19}H_{20}Cu_4I_4N_8$	$C_{24}H_{28}Cu_4I_4N_{10}$	$C_{11}H_{14}Cl_2N_4Zn$	$C_{20}H_{22}Cl_2N_8Zn$
M_W	1166.28	1122.19	1218.32	338.53	510.72
T / K	110	100	100	100	298
Crystal size / mm^3	0.02 × 0.25 × 0.31	0.20 × 0.10 × 0.05	0.50 × 0.46 × 0.02	0.40 × 0.30 × 0.08	0.20 × 0.13 × 0.10
Crystal system	Monoclinic	Monoclinic	Monoclinic	Triclinic	Triclinic
Space group	$C2/c$	$C2/c$	$P2_1/c$	$P-1$	$P-1$
a / Å	15.9272(8)	21.494(4)	18.283(5)	7.1708(4)	9.0863(3)
b / Å	9.0050(4)	8.331(1)	8.628(2)	8.4435(4)	9.2004(4)
c / Å	22.348(1)	18.367(3)	21.554(5)	12.2732(6)	14.2638(6)
α / °				91.226(1)	102.256(1)
β / °	102.105(1)	121.704(3)	97.845(5)	101.400(1)	94.334(1)
γ / °				111.390(1)	100.742(1)
V / Å^3	3134.0(3)	2798.2(8)	3368.2(15)	674.70(6)	1136.56(8)
Z	4	4	4	2	2
D_{calc} / g cm^{-3}	2.472	2.664	2.403	1.666	1.492
μ / mm^{-1}	6.645	7.437	6.191	2.202	1.340
θ range / °	1.86–33.23	2.23–27.50	1.12–27.50	1.70–28.30	1.47–27.89
Reflections collected	39341	9555	21954	24861	40402
Independent reflections [R_{int}]	5992 [0.0239]	3191 [0.0429]	7719 [0.0572]	3368 [0.0264]	5417 [0.0297]
Parameters	181	159	408	163	280
GOF	1.175	1.162	1.050	1.057	1.057
$R_1(I > 2\sigma(I))$	0.0276	0.0369	0.0526	0.0181	0.0261
wR_2(all data)	0.0555	0.1201	0.1462	0.0444	0.0690

Experimental reflections were collected with a Bruker AXS APEX diffractometer equipped with a CCD area-detector using Mo-K_α radiation (λ = 0.71073 Å).(Table 1) Collecting frames of data, indexing reflection and determination of lattice parameters and polarization effects were performed with the Bruker SMART.[30] The integration of intensity of reflections and scaling were carried out using Bruker SAINT.[30] The empirical absorption correction was performed by SADABS.[31] The space group determination, structure solution and least-squares refinements on $|F|^2$ were carried out with the Bruker SHELXL.[32] The structures were solved by direct methods to locate the heavy atoms, followed by difference maps for the light non-hydrogen atoms. Anisotropic thermal parameters were refined for the rest of the non-hydrogen atoms. The methyl group of ligand L1 in complex **1** shows disordered structures. One lattice CH_3CN molecule in complex **3** is disordered by flipping with an occupancy ratio of 83:17. Restraints in bond lengths and thermal parameters were applied to the disordered atoms. Hydrogen atoms were placed geometrically and refined isotropically. CCDC reference numbers: 1000337(**1**), 958913(**2**), 958914(**3**), 1034399(**4**) and 1034401(**5**).

Results and discussion

All ligands L1–L3 were prepared using CuAAC click synthetic conditions.[20–29] Molecular structures were confirmed by ^{1}H and ^{13}C NMR spectroscopy. The Cu(I) complexes **1–3** were prepared by layering the corresponding ligand solutions onto the CuI solution layer in test tubes. The Zn(II) complexes **4** and **5** were obtained by mixing the corresponding ligands with $ZnCl_2$ in methanol in test tubes. Crystals suitable for single-crystal XRD were obtained in about two weeks for all complexes **1–5**. All attempts to grow suitable single-crystal of the Zn(II) complex of L2 were unsuccessful. All complexes **1–5** have been analysed by microanalysis and infrared spectroscopy. Their powder samples were collected by filtration under vacuum and washed by the synthesis solvent (CH_3CN or CH_3OH) and Et_2O. There are lattice CH_3CN molecules in complex **3**, but partially lose occurs during sample collection and drying. The calculated formula $[Cu_4I_4(L3)]\cdot 0.7(CH_3CN)$ for powder sample (**3**) was estimated based on its elemental analytical data and TGA results. The BET surface area of **3** determined from N_2 adsorption–desorption measurement at 77 K was about 11.9 m^2/g. Degassing resulted in loss of crystallinity.

Crystal structure description

Complexes **1–3** are stair-step $[Cu_4I_4]$ cluster-based coordination complexes. The ligand L1 coordinates in a bidentate/monodentate fashion while ligands L2 and L3 display bis(bidentate/monodentate) binding. Interestingly, ligand L1 bridges Zn(II) centers in **4** using N_{py}-3'-N_{tri} links that yield a 1-D coordination polymer. Ligand L3, however, bridges Zn(II) centers using 3,3'–N_{tri} links to form 1-D coordination polymer **5**. Metal geometries are all tetrahedral with coordination environments of $Cu(N_{py}\text{-}2'\text{-}N_{tri})I_2$ and $Cu(3'\text{-}N_{tri})I_3$ in **1–3**, $Zn(N_{py})(3'\text{-}N_{tri})Cl_2$ in **4** and $Zn(3'\text{-}N_{tri})_2Cl_2$ in **5**.

Complex **1** crystallizes in the monoclinic crystal system with a space group of *C*2/*c* (Fig. 1). The asymmetric unit contains two Cu(I) centers, two bridging I^- ions and one L1 ligand. The Cu1 center is coordinated by two bidentate N donors from pyridine and 2'-triazole, one μ_2-I and one μ_3-I ligands. The Cu2 center is coordinated by one 3'-N_{tri} donor of L1 ligand, one μ_2-I and two μ_3-I ions. The Cu1···Cu2 and Cu2···Cu2 distances are 2.68 and 2.85 Å in the stair-step structure. Each $[Cu_4I_4]$ core is capped by two L1 ligands. The shortest intermolecular Cu···Cu distance is ~6.6 Å in the lattice of **1**.

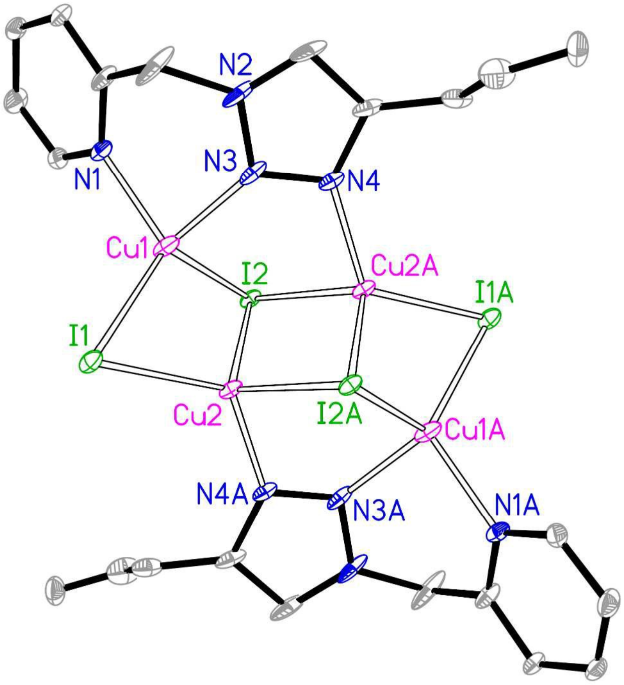

Fig. 1 Molecular structure of complex **1**.

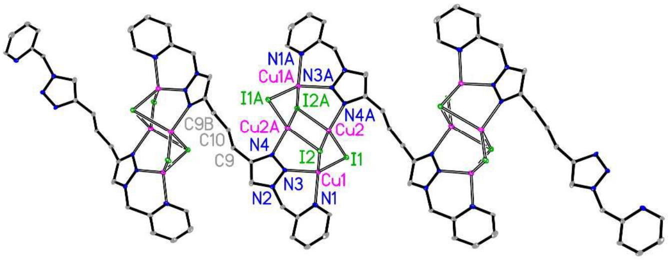

Fig. 2 1-D Molecular structure of complex **2**.

Complexes **2** and **3** crystallize in the monoclinic crystal system with space groups of *C*2/*c* and *P*2$_1$/*c*, respectively. The asymmetric unit of **2** contains two Cu(I) centers (Fig. 2) while the asymmetric unit of **3** contains four Cu(I) centers (Fig. 3a). The Cu1···Cu2 and Cu2···Cu2 distances are 2.64 and 2.71 Å in the stair-step $[Cu_4I_4]$ structure of **2**. The corresponding Cu···Cu distances in **3** are 2.641, 2.97 and 2.635 Å. The bis(bidentate/monodentate) ligands L2 and L3 containing methylene bridges ($-C_3H_6-$ and $-C_4H_8-$) afford the stair-step $[Cu_4I_4]$ cluster-based 1-D coordination polymers of **2** and **3**, respectively. The 1-D chains are parallel to each other in the lattice of **2** (Fig. 2). Remarkably, there are two series of linear chains extending in two directions ([011] and [01–1]) in the lattice of **3** (Fig. 3b). The packing of these polymeric chains generates 1-D channels along the *b* direction (Fig. 3c). Complex **3** is also a rare example of a linear coordination polymer with channel structures.[33] The intra-chain shortest Cu···Cu distances of neighbouring $[Cu_4I_4]$ cores are 7.7 Å in **2** and 11.2 Å in **3**, respectively.

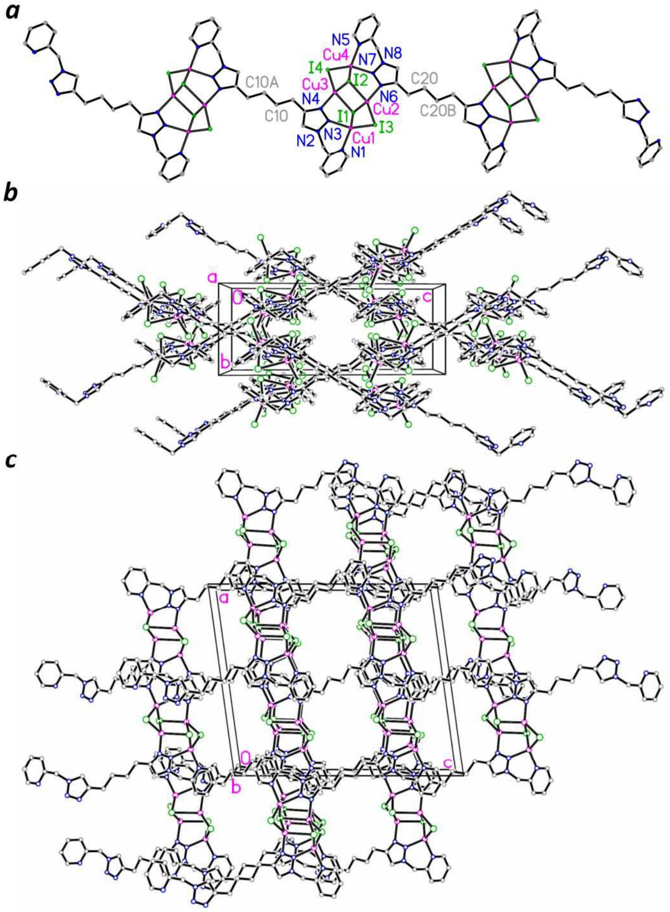

Fig. 3 (a) 1-D Molecular structure of complex **3**. (b), (c) Packing structures of different directions in complex **3**.

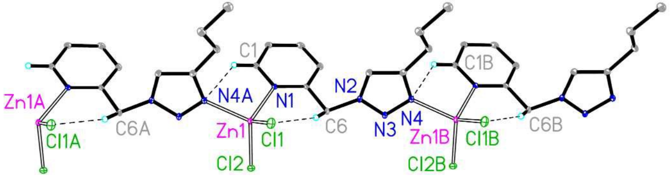

Fig. 4 1-D Molecular structure of complex **4** with intramolecular H-bonding interactions. (Only H atoms involved in H-bonding are included) Intra- and inter-molecular Zn···Zn distances are 8.4 and 6.8 Å respectively.

Complex **4** possesses a 1-D Zn(II) polymeric structure and crystallizes in the triclinic crystal system with a space group of *P*–1 (Fig. 4). Ligand L1 demonstrates an unusal bridging mode using the atoms of N_{py} and 3'-N_{tri}. This coordination is different to that observed in the Cu(I) complex **1** or that previously reported for the Pd(II) complex $[Pd(\eta^3\text{-}C_3H_5)(L1)]BF_4$ (**6**).[22] Each Zn(II) center in **4** is surrounded by two Cl^- ligands and two N donors (N_{py} and 3'-N_{tri}). There exist intra-chain C–H···N and C–H···Cl H-bonding interactions. The C–H···N H-bonds are formed between pyridine and triazole of neighbouring ligands. The C–H···Cl H-bonds are formed between methylene hydrogen and coordinated Cl^- ions(Fig. 4, Table 2). These H-bonds may explain the different mode of coordination observed for L1 in this complex, relative to that observed in complexes **1** and **6**. Both interactions stabilize a more open arrangement of the two N-donor heterocycles, with a relatively large dihedral angle (76.8°) between the pyridine and triazole rings, compared to the corresponding angles in complexes **1** (52.4°) or **6** (52.2°).

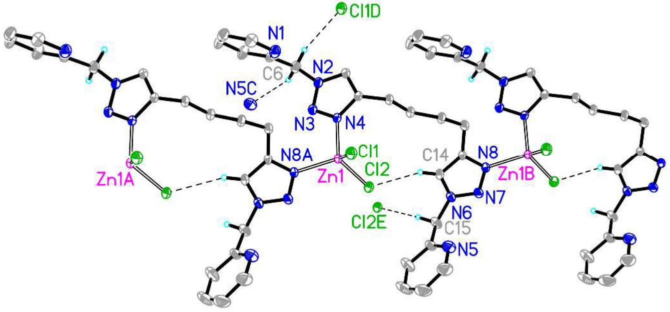

Fig. 5 1-D Molecular structure with intra- and inter-molecular H-bonding interactions in **5**. (Only H atoms involved in H-bonding are included) Intra- and inter-molecular Zn···Zn distances are 9.2 and 7.8 Å respectively.

Complex **5** crystallizes in the triclinic crystal system with a space group of *P*–1.(Fig. 5) Ligand L3 bridges the Zn(II) centers using 3,3'-N_{tri} donors to form a 1-D coordination polymer. Although with a different ligand, similar bridging was observed in the cyclic binuclear Zn(II) complex $[Zn_2Cl_4(L4)_2]$ (L4 = bis(4-(2-pyridylthiomethyl)-1*H*-1,2,3-triazolyl)pentane).[28] Again no chelation by the ligand in **5** is observed for reasons of intra-molecular C–H···Cl and inter-molecular C–H···Cl and C–H···N H-bonding interactions(Table 2). The dihedral angles between neighbouring pyridine and triazole rings in ligand L3 are 96.0 and 88.9°, larger than those (72.4 and 68.2°) for Cu(I) complex **3**.

Table 2 Hydrogen bond parameters in complexes **4** and **5**.

D–H···A	D–H (Å)	D···A (Å)	H···A (Å)	∠D–H···A (°)
		Complex **4**		
C1–H···N4A	0.95	3.203(2)	2.58	124
C6–H···Cl1	0.99	3.585(1)	2.63	162
Symmetry code A: *x*, *y*–1, *z*.				
		Complex **5**		
C14–H···Cl2	0.93	3.628(2)	2.75	157
C6–H···N5C	0.97	3.442(3)	2.54	155
C6–H···Cl1D	0.97	3.717(2)	2.77	165
C15–H···Cl2E	0.97	3.655(2)	2.72	162
Symmetry codes: C, *x*–1, *y*–1, *z*; D, *x*–1, *y*, *z*; E, 1–*x*, 2–*y*, 1–*z*.				

Analysis of structural motifs

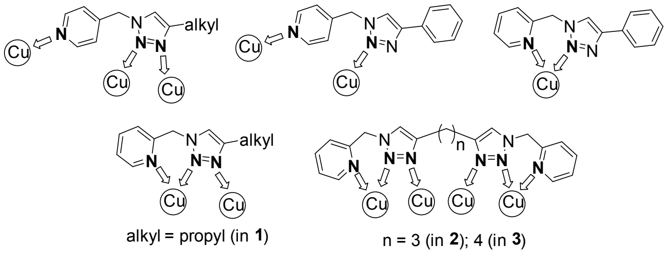

Scheme 2 Coordination modes in pyridyl-triazole copper complexes.

The coordination motifs of pyridyl-triazole copper complexes that we have observed in this work and previous studies are depicted in Scheme 2. In general, 4-pyridyl functionalized 1,2,3-triazoles with flexible alkyl (butyl, pentyl or hexyl) groups bind three Cu centers, each in a monodentate fashion to yield a 3-D coordination polymer with cubic [Cu_4I_4] clusters and [CuI]$_n$ polymeric structures.[25,26] By comparison, 4-pyridyl functionalized 1,2,3-triazole bearing a rigid phenyl group displays a bridging coordination mode by employing the N_{py} and 2'-N_{tri} donors to produce a [Cu_2I_2] rhombohedra based 1-D coordination polymer.[27] The analogous 2-pyridyl functionalized 1,2,3-triazole ligand L5 with a rigid (phenyl) group (L5 = 2-((4-phenyl-1*H*-1,2,3-triazol-1-yl)methyl)pyridine) exhibits a chelating mode in mononuclear Cu(II) complexes.[16,34] It indicates a monodentate coordination using the N-donor of pyridine in the Cu(II) complex [$Cu_2(L5)_2(OAc)_4$]·$4CH_3CN$.[35] However, a 2-pyridyl functionalized 1,2,3-triazole with a flexible (hexyl) group displays a mixed bidentate/monodentate coordination mode to produce a magnetic binuclear Cu(II) complex.[36] In this work, 2-pyridyl functionalized 1,2,3-triazole (L1) with a flexible propyl group also displayed a mixed bidentate/monodentate mode of coordination to form a step-stair Cu_4I_4 cluster structure(**1**). The bis(2-pyridyl-triazole) ligands L2 and L3 with flexible methylene bridges ($-C_3H_6-$ or $-C_4H_8-$) exhibit bis(bidentate/monodentate) coordination to produce step-stair [Cu_4I_4] cluster based 1-D coordination polymers (**2** and **3**). This is made possible by the spacer that not only supports the [Cu_4] cluster but as the key polymeric connector. They are thus among the most valuable spacers for the self-assembly of polymers-of-oligomers frameworks.[25,37]

Diverse coordination modes with phenyl substituted ligand L5 have been observed for complexes of other metal salts. With silver precursors, for example, L5 adopts a bidentate/monodentate coordination mode to yield a trinuclear Ag^+ cationic complex and a dinuclear Ag(I) complex [$Ag_2(L5)_2(NO_3)_2$].[34,38] Mercury bromide also combines with L5 to produce a 1-D Hg(II) coordination polymer [$Hg_4Br_8(L5)_2$]$_n$ involving mixed bidentate/monodentate coordination.[39] However, bidentate coordination is observed for the Pd(II) complex [$Pd(L5)_2$]$(BF_4)_2$·$2CH_3CN$, Pt(II) complex [$PtCl_2(L5)$] and Ru(II) complex [RuCl(η^6-*p*-cymene)(L5)]OTf.[34] Monodentate coordination using the N-donor of pyridine or triazole has been reported for the Pd(II) complex [$PdCl_3(HL5)$]·H_2O and Rh(II) complex [$Rh_2(O_2CCH_3)_4(L5)_2$].[39] Clearly then, the same ligand with different metals and metal geometries can generate quite different structures. DFT calculations for L5 indicate that the $N_{2\text{-}py}$ is the most electron rich donor atom, followed by N3' and then N2' of the triazole.[34,39] Flexibility of the ligand and the pendant group is also important for determining the mode of coordination, particularly for the copper(I) iodide cluster complexes.

There are less examples of the corresponding Zn(II) complexes, however some trends can be discerned. Both 4-pyridyl-triazoles with flexible alkyl (butyl, pentyl or hexyl) groups and 2-pyridyl-triazole with a propyl group (L1) bridge *via* N_{py} and 3'-N_{tri} to yield 1-D coordination polymers (eg **4**). The bis(pyridyl-triazole) ligands employed here also bridge the Zn(II) centers using 3,3'-N_{tri} atoms in the cyclic Zn(II) binuclear complex[28] and 1-D coordination polymer of **5**. In the latter case, it frees up the pyridyl nitrogen to potentially capture other acidic metal fragments and provide multimetallic modalities.

Powder XRD, TGA and photoluminescence

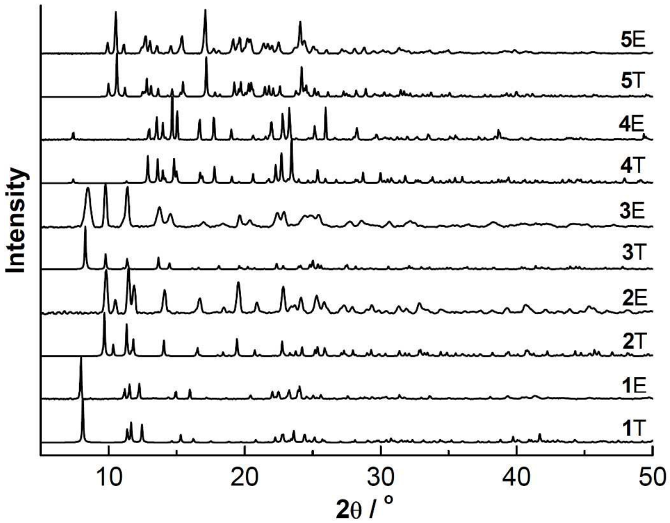

Fig. 6 Powder XRD patterns of complexes **1–5** (T = theoretical profile referenced to the experimentally determined structure by single-crystal XRD; E = experimental data).

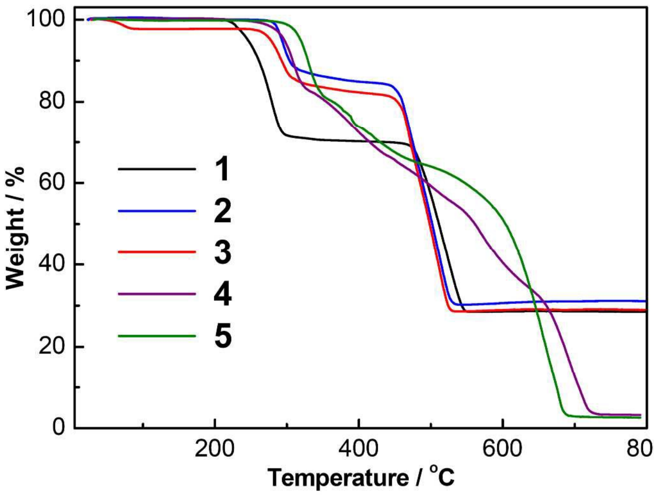

Fig. 7 TGA curves of complexes **1–5**.

Complexes **1–5** were structurally characterized by single-crystal X-ray diffractions. The experimental powder X-ray diffraction patterns of as prepared samples matched the simulated patterns, supporting their phase purity (Fig. 6). We suspect that broadness observed in some pattens is due to solvent los during drying and handling. The thermogravimetric analysis (TGA) curves of complexes **1–5** from room temperature to 800°C are given in Fig. 7. During the heating process, complexes **1–5** are stable to ~200, 270, 250, 250 and 280°C, respectively, followed by steady declines until reaching residual weights at ~550, 540, 540, 730 and 700°C. Complexes **2** and **3** were slightly more stable than complex **1** presumably due to the polymeric nature of these compounds.

The photoluminescent properties of ligands L1–L3 in solution and of complexes **1–5** in the solid state have been investigated. The normalized excitation and emission spectra are given in Figs. 8 and 9. Ligands L1–L3 displayed broad excitation spectra between 280–420 nm with maximum wavelengths at ~346, 344 and 346 nm, respectively. Excitation at these wavelengths resulted in broad emission spectra between 360–575 nm with maximum wavelength at ~438, 432 and 430 nm, respectively. The ligands' emissions can be assigned to intraligand transitions.

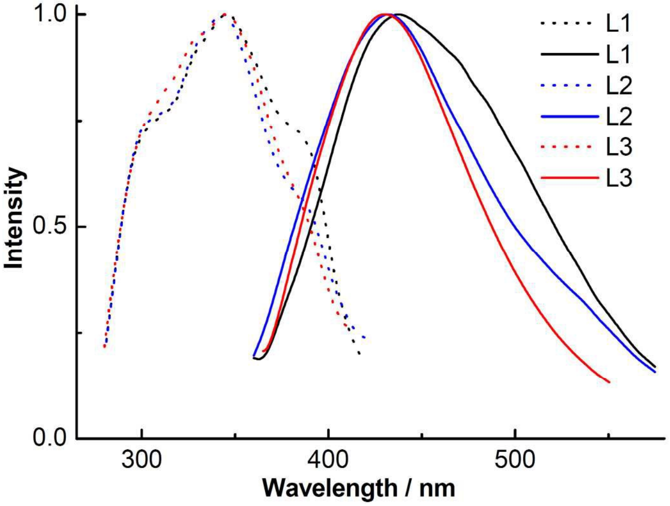

Fig. 8 Normalized solution excitation (dotted line) and emission (solid line) spectra of ligands L1–L3.

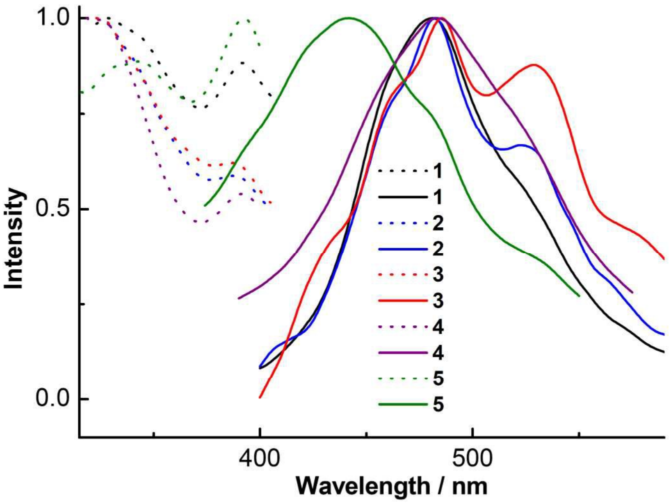

Fig. 9 Normalized solid state excitation (dotted line) and emission (solid line) spectra of complexes **1–5**.

The excitation spectra of these complexes have maxima at 327, 327 and 324 nm respectively, which give strong broad emissions with maximum wavelengths at ~481, 482 and 485 nm, respectively. These luminescent emissions are slightly different from those of the bis(benzyl-1,2,3-triazole) tetranuclear copper(I) iodide complexes (emission between 400–700 nm with maximum wavelengths between 495–524 nm (Cu···Cu, 2.53–2.75 Å)).[40] Based on the Cu···Cu distances (2.64–2.97 Å) within the stair-step $[Cu_4I_4]$ structures, the emissions of complexes **1–3** are attributed to metal-to-ligand charge-transfer, iodide-to-ligand charge transfer, cluster-centered transitions, or combined excited states of these luminophores.[40,41]

The Zn(II) complexes absorb at ~326 and 394 nm for complex **4** and 345 and 394 nm for complex **5**. On excitation at 394 and 345 nm, complexes **4** and **5** gave strong broad emission spectra with maximum wavelength at ~483 and 441 nm, respectively. These emissions can be assigned to intraligand transitions and/or metal-to-ligand-charge-transfer states. The difference (~42 nm) of their emission maxima may be due to the difference in Zn(II) coordination environments ($Zn(N_{py})(N_{tri})Cl_2$ in **4** and $Zn(N_{tri})_2Cl_2$ in **5**).

Conclusions

This work reports three luminescent copper(I) iodide and two zinc(II) complexes being supported by 2-pyridyl-1,2,3-triazole ligands. It provides the opportunity to systematically compare the structural types, coordination modes and substituent effects of complexes **1–5** with analogues reported previously and thereby develop structural relationships. The rare bridging mode of ligand L1 in Zn(II) complex **4** exemplifies the diversity of coordination modes and molecular structures available with subtle changes in substituent. Weak H-bonding interactions also play an important role and could potentially be designed to tune the coordination mode, luminescence and other molecular properties.

Acknowledgements

We are grateful to Dr. L. L. Koh, G. K. Tan and Y. M. Hong for X-ray diffractometry measurement assistance. We acknowledge the financial support (IMRE/12-1P0907 and IMRE/14-1C0248) by the Institute of Materials Research and Engineering of A*STAR of Singapore and the National University of Singapore.

Notes and references

[a] *Institute of Materials Research and Engineering, A*STAR (Agency for Science, Technology and Research), 3 Research Link, Singapore 117602, Republic of Singapore. Tel: (65) 65141515, E-mail: bais@imre.a-star.edu.sg; andyhor@imre.a-star.edu.sg.*
[b] *Department of Chemistry, National University of Singapore, 3 Science Drive 3, Singapore 117543, Republic of Singapore.*
[c] *School of Science, Monash University, 47500, Bandar Sunway, Selangor D.E., Malaysia.*

† *Electronic supplementary information (ESI) available. CCDC 1000337(**1**), 958913(**2**), 958914(**3**), 1034399(**4**) and 1034401(**5**).*

1 V. W.-W. Yam and K. K.-W. Lo, *Chem. Soc. Rev.*, 1999, **28**, 323–334.
2 M. Vitale and P. C. Ford, *Coord. Chem. Rev.*, 2001, **219–221**, 3–16.
3 K. K.-W. Lo, A. W.-T. Choi and W. H.-T. Law, *Dalton Trans.*, 2012, **41**, 6021–6047.
4 Z. Liu, W. He and Z. Guo, *Chem. Soc. Rev.*, 2013, **42**, 1568–1600.
5 H. Xu, R. Chen, Q. Sun, W. Lai, Q. Su, W. Huang and X. Liu, *Chem. Soc. Rev.*, 2014, **43**, 3259–3302.
6 T. Gunnlaugsson, M. Glynn, G. M. Tocci (née Hussey), P. E. Kruger, F. M. Pfeffer, *Coord. Chem. Rev.*, 2006, **250**, 3094–3117.
7 X.-C. Shan, F.-L. Jiang, D.-Q. Yuan, H.-B. Zhang, M.-Y.Wu, L. Chen, J. Wei, S.-Q. Zhang, J. Pan and M.-C. Hong, *Chem. Sci.*, 2013, **4**, 1484–1489.
8 A. J. Blake, N. R. Brooks, N. R. Champness, L. R. Hanton, P. Hubberstey and M. Schröder, *Pure Appl. Chem.*, 1998, **70**, 2351–2357.
9 C. H. Arnby, S. Jagner and I. Dance, *CrystEngComm*, 2004, **6**, 257–275.
10 W.-P. Leung, C.-W. So, K.-H. Chong, K.-W. Kan, H.-S. Chan and T. C. W. Mak, *Organometallics,* 2006, **25**, 2851–2858.
11 Y. Chen, H.-X. Li, D. Liu, L.-L. Liu, N.-Y. Li, H.-Y. Ye, Y. Zhang and J.-P. Lang, *Cryst. Growth Des.* 2008, **8**, 3810–3816.
12 R. Visbal and M. C. Gimeno, *Chem. Soc. Rev.*, 2014, **43**, 3551–3574.
13 V. V. Rostovtsev, L. G. Green, V. V. Fokin and K. B. Sharpless, *Angew. Chem., Int. Ed.*, 2002, **41**, 2596–2599.

14 C. W. Tornøe, C. Christensen and M. Meldal, *J. Org. Chem.*, 2002, **67**, 3057–3064.

15 M. Meldal and C. W. Tornøe, *Chem. Rev.*, 2008, **108**, 2952–3015.

16 W. S. Brotherton, H. A. Michaels, J. T. Simmons, R. J. Clark, N. S. Dalal and L. Zhu, *Org. Lett.*, 2009, **11**, 4954–4957.

17 J. D. Crowley and D. A. McMorran, *Top. Heterocycl. Chem.*, 2012, **28**, 31–84.

18 D. Schweinfurth, N. Deibel, F. Weisser and B. Sarkar, *Nachr. Chem.*, 2011, **59**, 937–941.

19 H. Struthers, T. L. Mindt and R. Schibli, *Dalton Trans.*, 2010, **39**, 675–696.

20 J. E. Hein and V. V. Fokin, *Chem. Soc. Rev.*, 2010, **39**, 1302–1315.

21 J. D. Crowley and P. H. Bandeen, *Dalton Trans.*, 2010, **39**, 612–623.

22 E. Amadio, A. Scrivanti, G. Chessa, U. Matteoli, V. Beghetto, M. Bertoldini, M. Rancan, A. Dolmella, A. Venzo and R. Bertani, *J. Organomet. Chem.*, 2012, **716**, 193–200.

23 B. Schulze and U. S. Schubert, *Chem. Soc. Rev.*, 2014, **43**, 2522–2571.

24 S.-Q. Bai, S. Leelasubcharoen, X. Chen, L. L. Koh, J.-L. Zuo and T. S. A. Hor, *Cryst. Growth Des.*, 2010, **10**, 1715−1720.

25 S.-Q. Bai, J. Y. Kwang, L. L. Koh, D. J. Young and T. S. A. Hor, *Dalton Trans.*, 2010, **39**, 2631–2636.

26 S.-Q. Bai, A. M. Yong, J. J. Hu, D. J. Young, X. Zhang, Y. Zong, J. Xu, J.-L. Zuo and T. S. A. Hor, *CrystEngComm*, 2012, **14**, 961–971.

27 S.-Q. Bai, L. Jiang, J.-L. Zuo and T. S. A. Hor, *Dalton Trans.*, 2013, **42**, 11319–11326;

28 L. Jiang, Z. Wang, S.-Q. Bai and T. S. A. Hor, *CrystEngComm*, 2013, **15**, 10451–10458.

29 L. Jiang, Z. Wang, S.-Q. Bai and T. S. A. Hor, *Dalton Trans.*, 2013, **42**, 9437–9443;

30 *SMART & SAINT Software Reference Manuals*, Bruker AXS GmbH, Karlsruhe, Germany, 2000.

31 L. Krause, R. Herbst-Irmer, G. M. Sheldrick and D. Stalke, *J. Appl. Cryst.*, 2015, **48**, 3.

32 G. M. Sheldrick, *Acta Cryst.*, 2015, **C71**, 3–8.

33 E. Y. Lee and M. P. Suh, *Angew. Chem. Int. Ed.*, 2004, **43**, 2798–2801.

34 D. Urankar, B. Pinter, A. Pevec, F. D. Proft, I. Turel and J. Košmrlj, *Inorg. Chem.*, 2010, **49**, 4820–4829.

35 P. M. Guha, H. Phan, J. S. Kinyon, W. S. Brotherton, K. Sreenath, J. T. Simmons, Z. Wang, R. J. Clark, N. S. Dalal, M. Shatruk and L. Zhu, *Inorg. Chem.*, 2012, **51**, 3465−3477.

36 S.-Q. Bai, L. Jiang, J.-L. Zuo, C.-H. Yan and T. S. A. Hor, *Aust. J. Chem.* 2013, **66**, 1029–1033.

37 P. Teo, L. L. Koh and T. S. A. Hor, *Inorg. Chem.*, 2008, **47**, 9561–9568.

38 J. D. Crowley, P. H. Bandeen and L. R. Hanton, *Polyhedron*, 2010, **29**, 70–83.

39 D. Urankar, A. Pevec, I. Turel and J. Košmrlj, *Cryst. Growth Des.*, 2010, **10**, 4920–4927.

40 G. F. Manbeck, W. W. Brennessel, C. M. Evans and R. Eisenberg, *Inorg. Chem.*, 2010, **49**, 2834–2843.

41 F. De Angelis, S. Fantacci, A. Sgamellotti, E. Cariati, R. Ugo and P. C. Ford, *Inorg. Chem.*, 2006, **45**, 10576–10584.

Graphical Abstract

Five Cu(I) and Zn(II) clusters and coordination polymers of 2-pyridyl-1,2,3-triazoles: synthesis, structures and luminescent properties

Shi-Qiang Bai,* Lu Jiang, Bin Sun, David James Young and T. S. Andy Hor*

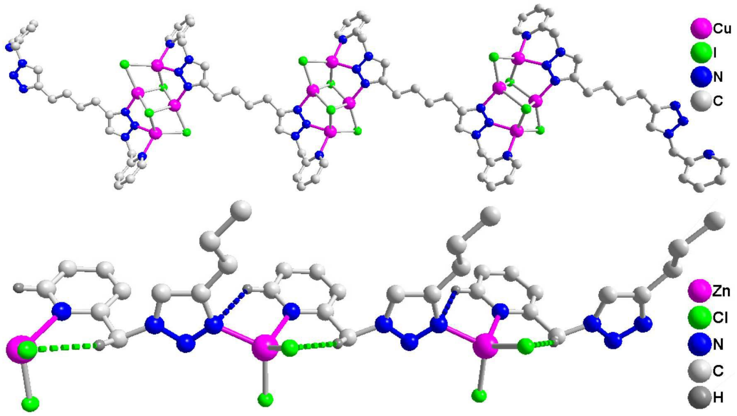

2-Pyridyl-1,2,3-triazoles with flexible substituent demonstrate rare coordination modes and support new luminescent clusters and coordination polymers.